A NEW BROWN DWARF DESERT? A SCARCITY OF WIDE ULTRACOOL BINARIES

Peter R. Allen
Department of Astronomy and Astrophysics, Pennsylvania State University, University Park, PA, USA; pallen@astro.psu.edu

David W. Koerner
Department of Physics and Astronomy, Northern Arizona University, Flagstaff, AZ, USA; koerner@physics.nau.edu

Michael W. McElwain
Department of Physics and Astronomy, UCLA, Los Angeles, CA, USA; mcelwain@astro.ucla.edu

Kelle L. Cruz
Department of Astrophysics, American Museum of Natural History, New York, NY, USA; kelle@amnh.org

AND

I. Neill Reid
Space Telescope Science Institute, Baltimore, MD, USA; inr@stsci.edu

ABSTRACT

We present the results of a deep-imaging search for wide companions to low-mass stars and brown dwarfs using NSFCam on the Infrared Telescope Facility. We searched a sample of 132 M7–L8 dwarfs to magnitude limits of $J \sim 20.5$ and $K \sim 18.5$, corresponding to secondary-to-primary mass ratios of ~ 0.5. No companions were found with separations between $2''$ and $31''$ (~ 40 to ~ 1000 AU). This null result implies a wide companion frequency below 2.3% at the 95% confidence level within the sensitivity limits of the survey. Preliminary modeling efforts indicate that we could have detected 85% of companions more massive than 0.05 $M_\odot$ and 50% above 0.03 $M_\odot$.

Key words: binaries: general — stars: low-mass, brown dwarfs

Online material: color figure, machine-readable table

1. INTRODUCTION

Low-mass stars and brown dwarfs are likely to be the most numerous constituents of the solar neighborhood. Over the last few years, several major surveys for these objects have been undertaken, aimed at measuring their numbers and discovering their origins. More than 350 L dwarfs and as many late-type M dwarfs have been discovered as a result of these projects (Delfosse et al. 1999; Kirkpatrick et al. 2000; Fan et al. 2000; Cruz et al. 2003; Phan-Bao et al. 2003). The current consensus is that the increasing number of objects per unit mass seen in high- and intermediate-mass stars begins to flatten noticeably near the substellar limit, 0.08 $M_\odot$ (Kroupa 2002; Burgasser 2004; Allen et al. 2005).

The origin of these low-mass ultracool dwarfs remains in question. The standard scenario envisions brown dwarfs forming in isolation, like higher mass stars, with the lower mass of the final product reflecting the smaller reservoir of material. However, a recent suggestion is that ultracool dwarfs have low masses because they are ejected from small stellar groups (Reipurth & Clarke 2001), rather than forming in isolation, as theorized for higher mass stars. This removes low-mass prestellar cores from the star-forming cloud, truncating the accretion process and leading to the formation of very low mass stars or brown dwarfs.

The frequency of ultracool binary systems and the distribution of their properties (mass ratios, separations, orbital eccentricities, etc.) provide constraints on formation models. The ejection scenario, for example, predicts a low binary frequency and few, if any, wide systems. High spatial resolution observations, with both the *Hubble Space Telescope* (Martín et al. 1998; Reid et al. 2001; Gizis et al. 2003; Burgasser et al. 2003; Bouy et al. 2003) and ground-based high-resolution cameras and adaptive optics systems (Koerner et al. 1999; Close et al. 2003; Siegler et al. 2003),

have shown that $\sim 20\%$ of ultracool dwarfs are binary systems. None of these binaries has a separation that exceeds 15 AU. Only one field ultracool dwarf system has been discovered to date with a separation greater than 15 AU (Billères et al. 2005). This is in contrast to ultracool dwarfs with higher mass primaries: VB 10, for example, the archetypal late-type M dwarf, lies 400 AU from its primary, the M3 dwarf Gl 752A (van Biesbroeck 1944), while the nearby T dwarfs Gl 229B, Gl 570D, and ϵ Indi Bab are all wide components in multiple systems. A handful of wide, *young* ultracool binaries have been discovered. Luhman (2004) has identified a pair of late-type M dwarfs separated by 240 AU in ρ Ophiuchus, Close et al. (2006) found an additional 212 AU binary in Ophiuchus and Chauvin et al. (2004) have discovered a very low mass brown dwarf companion of the TW Hya member 2M 1207, with a separation of 60 AU.

This paper describes our survey to determine whether there are any wide ultracool dwarf binary systems in the field. We obtained deep, multiepoch J and K images of 132 isolated dwarfs with spectral types from M7 to L8 to an absolute J-band magnitude of ~ 17.5. We searched for candidate companions using photometric criteria to verify the nature of those candidates. Section 2 details the target selection, the imaging observations, and the reduction and analysis of the imaging data; § 3 describes the candidate selection process and follow-up observations; and § 4 summarizes our results and discusses their implications.

2. TARGET SELECTION, OBSERVATIONS, AND DATA REDUCTION

2.1. *Target Selection and Sample Information*

Our sample is a subset of the first ultracool dwarf surveys (Kirkpatrick et al. 1997, 1999, 2000; Gizis et al. 2000; Delfosse
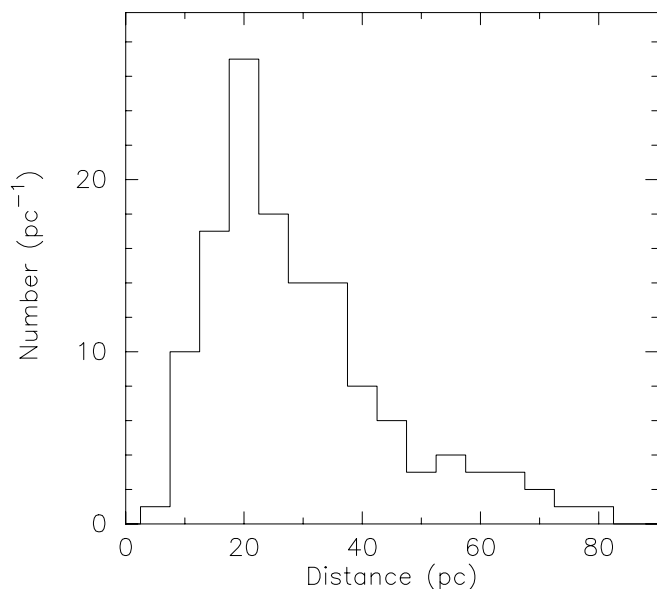
FIG. 1.—Histogram of the distance estimates for all 132 target primaries in our IRTF sample. Estimates were obtained through a combination of trigonometric parallaxes (Dahn et al. 2002) and calibrated spectrophotometric relations (Cruz et al. 2003).
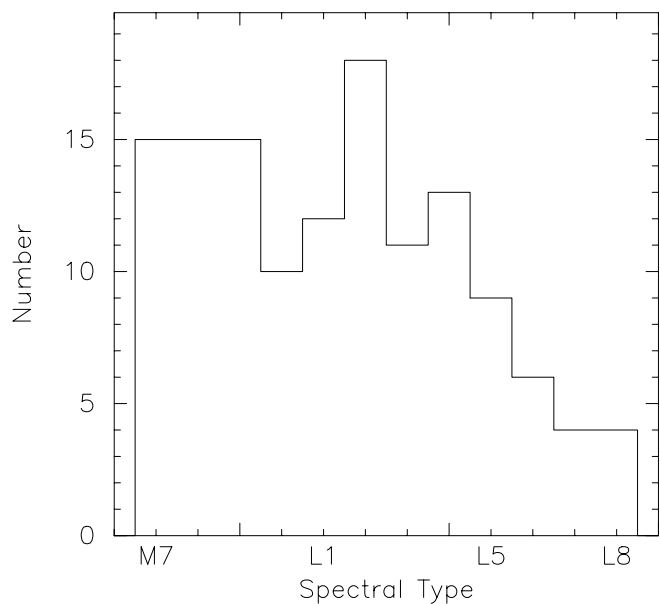

FIG. 2.—Histogram of the spectral types for all 132 target primaries in our IRTF sample. Spectral types were obtained from initial discovery papers (see Table 1).

et al. 1999; Fan et al. 2000). Those initial surveys tended to concentrate on brighter candidates, particularly in follow-up observations of extremely red DENIS and Two Micron All Sky Survey sources. As a result, our sample is effectively magnitude-limited and is therefore likely to include a higher proportion of unresolved close binary systems than a volume-limited sample (Burgasser et al. 2003). This bias is not directly relevant to the prime purpose of the present survey, which aims to determine the frequency of wide companions to ultracool dwarfs.

Figure 1 displays the distance estimates of the 132 targets observed in the present program. Those distances are based primarily on the spectroscopic parallaxes of Cruz et al. (2003), although a few objects have trigonometric parallax measurements (see § 3). Most candidates are within 30 pc of the Sun. Figure 2 shows the spectral type distribution, which is essentially flat from late-M to mid-L. The drop in numbers at later types reflects the relatively small numbers of those objects in the initial surveys. Thus, while the target sample is not statistically complete, it is representative of the nearby ultracool dwarf population.

2.2. *IRTF Data*

We observed all 132 targets using NSFCam on NASA's Infrared Telescope Facility (IRTF; Shure et al. 1994). The initial observations were obtained over four epochs, 2000 August, 2001 May, 2001 October, and 2002 February. We imaged each target at least once in both the J and K bands (Table 1). The largest pixel scale available on NSFCam, $0.3''$ pixel^{-1}, was used to provide a field of view of $76'' \times 76''$. This large field enabled the detection of ultracool companions to separations up to 1000 AU for our nearest targets. Each target was observed using two to three sets of five dither positions to allow for sky background subtraction and to minimize the effects of sky variability and detector defects.

We reduced the NSFCam data using IDL and IRAF routines. The five dither positions were subtracted, shifted, and combined to create a background-subtracted composite image. Finally, if there were multiple sets of dithers, we added the composite images together to create a final image. Candidates were limited to have separations from their primary between $2''$ and $35'' - 40''$ on aver-

age. The outer limit is set by the edge of the image and the inner limit by the size of the point-spread function (PSF) of the primary. We identified candidates by eye and obtained relative photometry of each object in the field from the final composite images using the *qphot* script within IRAF. The relative magnitudes of each source were estimated using published magnitudes of the target primaries (references are listed in Table 1).

We inserted faint artificial point sources uniformly across each composite image to determine its sensitivity. Each image was searched for these sources by eye. We found that the sensitivity of the array is uniform from outside the PSF of the primary ($\sim 2''$) almost to the edge of the chip ($\sim 38''$). However, we also discovered that our initial data reduction procedures introduced artifact sources into the outer $7''$ of each image. As a result, we revised the outer limit of our survey inward to $31''$ and rejected any candidates with larger projected separations. We therefore assign each final composite image a uniform detection limit out to $31''$.

Figure 3 shows the distribution of apparent magnitude limits in J and K for the survey fields; the median limiting magnitudes are $J = 20.5$ and $K = 18.5$. Figure 4 shows these limits expressed as companion detection limits (ΔJ, ΔK), the magnitude difference between the target and the detection limit. Finally, Figure 5 transforms these sensitivity limits to the absolute magnitudes of potential secondary companions, where we show the location of Gl 229B as a reference. Clearly, our observations extend well into the T dwarf regime and beyond in all cases. In general, the sensitivity at J is better than at K (particularly for neutral colored T dwarfs). The K-band limits listed in Table 1 therefore represent a conservative estimate of the sensitivity of our survey.

2.3. *WIYN Data*

Deep I-band images were obtained of a number of targets using the Mini-Mosaic Camera (Saha et al. 2000) on the WIYN telescope at Kitt Peak National Observatory. The observations were made in 2002 August and 2003 February. Conditions were adequate, with a seeing of $0.75'' - 1''$. While the August run was not photometric, the M and L dwarf targets provide an approximate local zero point that is sufficiently accurate to separate background

TABLE 1
IRTF OBSERVATIONS

Name	J	K_s	Spectral Type	Distance[a] (pc)	$m_{J_{\lim}}$	$m_{K_{\lim}}$	IRTF Obs. Date	Ref.
2M 0010+17	13.88 ± 0.03	12.81 ± 0.03	M8	35.1	21.38	18.56	2001 Oct	1
2M 0015+35	13.82 ± 0.04	12.81 ± 0.03	L2	20.1	19.57	20.31	2000 Aug	3
2M 0028+15	16.49 ± 0.14	15.33 ± 0.13	L4.5	43.3	20.41	21.08	2000 Aug	3
2M 0030−14..............	16.79 ± 0.16	15.36 ± 0.09	L7	29.7	20.71	19.72	2000 Aug	3
2M 0036+18	12.44 ± 0.04	11.58 ± 0.03	L3.5	8.8*	20.69	19.83	2000 Aug	3
2M 0051−15..............	15.23 ± 0.05	14.15 ± 0.05	L3.5	29.7	20.98	19.90	2000 Aug	3
2M 0058−06..............	14.32 ± 0.03	13.45 ± 0.04	L0	33.0	20.07	19.20	2000 Aug	3
2M 0103+19	16.26 ± 0.09	14.88 ± 0.07	L6	28.3	20.18	19.88	2000 Aug	3
2M 0104+14	13.70 ± 0.02	12.66 ± 0.03	M8	32.2	21.23	19.93	2000 Aug	1
2M 0105+14	13.59 ± 0.02	12.55 ± 0.03	M7	37.3	19.34	18.30	2001 Oct	1

NOTES.—Table 1 is published in its entirety in the electronic edition of the *Astronomical Journal*. A portion is shown here for guidance regarding its form and content.

[a] An asterisk indicates a distance derived from trigonometric parallaxes in Dahn et al. (2002).

REFERENCES.— (1) Gizis et al. 2000; (2) Kirkpatrick et al. 1999; (3) Kirkpatrick et al. 2000; (4) Cruz et al. 2003; (5) Kirkpatrick et al. 1997; (6) Dahn et al. 2002; (7) Delfosse et al. 1999; (8) Martín et al. 1999; (9) Fan et al. 2000; (10) Hawley et al. 2002.
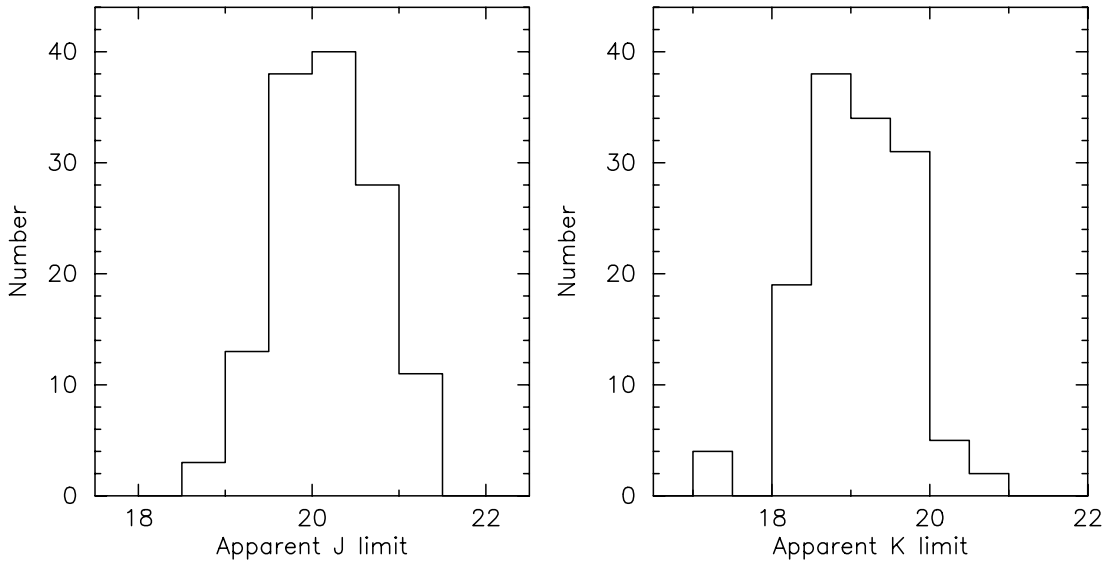

FIG. 3.—Histograms of the apparent J (*left*) and K (*right*) limiting magnitudes of the 132 first-epoch NSFCam fields.
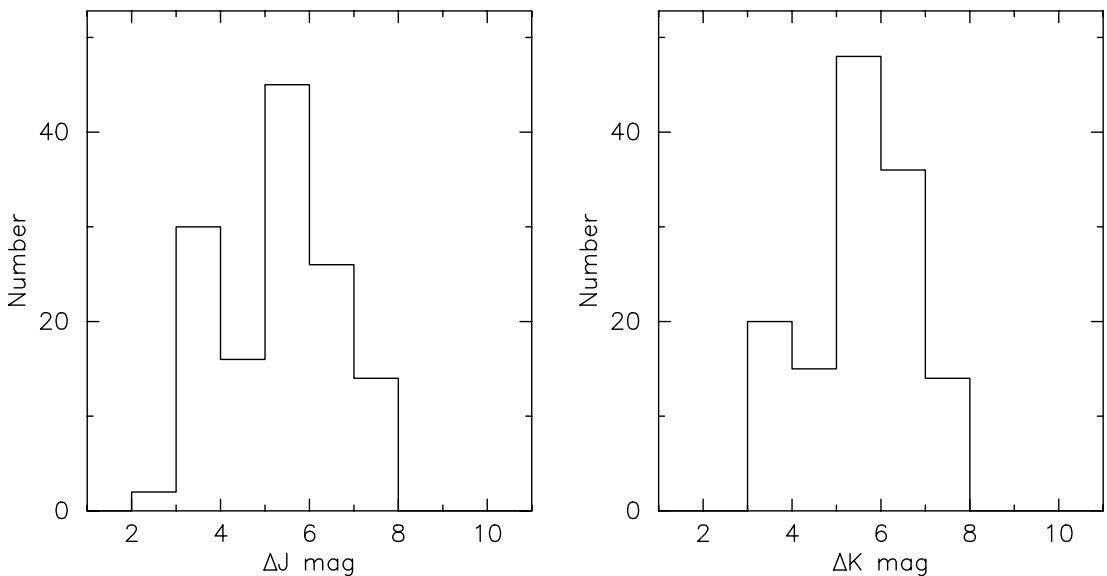

FIG. 4.—Histograms of the ΔJ (*left*) and ΔK (*right*) companion detection limits of the 132 first-epoch NSFCam fields. We obtained the Δ magnitudes by subtracting the magnitude of the target from the detection limit of each field.
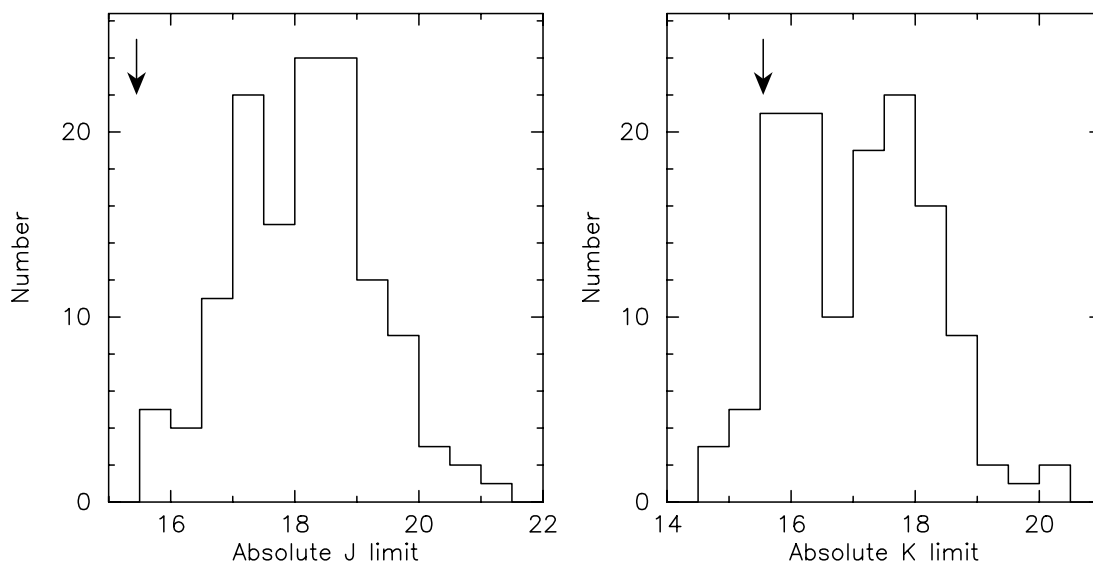
Fig. 5.—Histograms of the *J* (*left*) and *K* (*right*) limiting absolute magnitudes of the 132 first-epoch NSFCam fields. The position of the archetypal T dwarf Gl 229B is indicated with an arrow in both plots.

objects from real companions, as discussed in § 3. We used exposure times of 300 s, achieving typical limiting magnitudes for these observations of $I \sim 22.5$–23.

The images from the Mini-Mosaic Camera have a much larger field of view than the IRTF data. We trimmed and rotated each frame to match the NSFCam field. The relative photometry is based on the *I* magnitudes estimated for the M and L dwarf primaries from $I - J$ colors given in Figure 4 of Dahn et al. (2002). We estimated the *I* magnitudes because few of our targets have published photometry in the *I* band. The relative photometry was measured in the same manner used for the NSFCam data (*qphot*).

3. CANDIDATE COMPANION SELECTION

3.1. *Near-Infrared Criteria*

The candidate selection method was a multistep process. The initial step used the $M_J, J - K$ color-magnitude diagram. Figure 6 plots data for M, L, and T dwarfs with known trigonometric parallaxes. We have used those objects to delineate the regions of the $M_J, J - K$ plane in which we would expect to find low-luminosity companions to the ultracool targets. L dwarfs have colors redder than $J - K = 1$, and are brighter than $M_J \sim 15.5$; classical T dwarfs are bluer than $J - K = 0.5$ and fainter than $M_J = 14$; and transitional, early-type T dwarfs have intermediate colors, and $14 < M_J < 15.5$.

We identify candidate companions by plotting color-magnitude data for each infrared source as if it were at the same distance as the appropriate ultracool target. We use a M_J versus spectral type relation to derive distances to all the target primaries that lack a trigonometric parallax. This is the vast majority of our sample; only 6 of 132 have trigonometric parallax measurements. The Cruz et al. (2003) relation has distances uncertainties of $\sim 10\%$, which corresponds to an uncertainty of $\sim \pm 0.2$ mag. If the source falls between the dashed and dotted lines plotted in Figure 6, then it is a potential low-luminosity companion. A total of 221 sources meet these criteria.

3.2. *Optical Criteria*

Once the infrared candidates are selected, we cross-reference each against the POSS and UK Schmidt Telescope blue and red plates, as scanned in the Digitized Sky Survey (DSS; Djorgovski

et al. 2003). These photographic plates have limiting magnitudes of $B \sim 22$ and $R \sim 21$, while cool L and T dwarfs have extremely red optical-to-infrared colors, $(R - J) > 6$ (Golimowski et al. 1998). Thus, any sources visible on the DSS scans can be ruled out as candidate companions. Thirty-six objects pass this criterion (see Fig. 6), with colors consistent with late-L and T dwarfs.

Twenty-four of these remaining candidates were then observed at WIYN (Table 2). With *I*-band observations of these objects, a new dimension is added to the color analysis. In Figure 4 of Dahn et al. (2002) it is shown that dwarfs with spectral types of
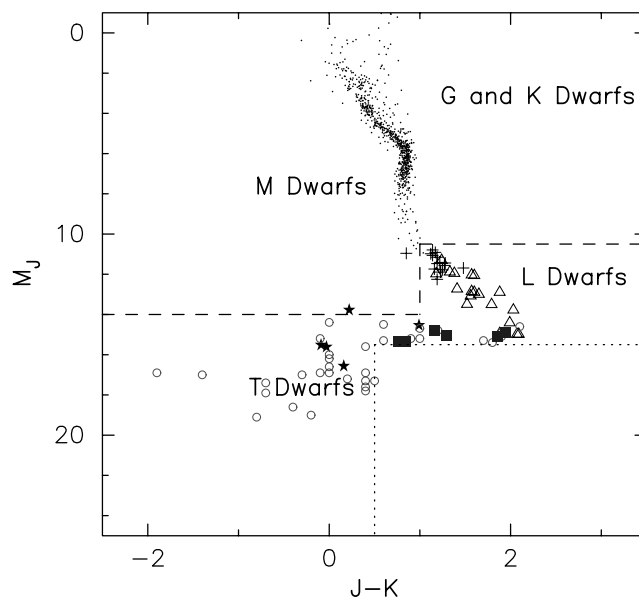

Fig. 6.—M_J vs. $J - K$ color magnitude diagram for nearby stars with trigonometric parallaxes: GKM dwarfs are shown as small dots, ultracool M dwarfs as crosses, L dwarfs as open triangles, and T dwarfs as five-pointed stars. The M_J and $J - K$ selection criteria for candidate companions are shown as dashed and dotted lines, respectively. All sources that fall between those lines are accepted as initial candidates and are checked against the POSS plates. The 36 objects that passed both criteria are plotted as open circles at an absolute *J* magnitude that is consistent with the same distance as their putative primaries. The six remaining candidates are marked as squares. [*See the electronic edition of the Journal for a color version of this figure.*]

TABLE 2
Color-Selected Candidate Companions

Name	Spectral Type (Primary)	$M_{J_{sec}}$	$J - K_{sec}$	Distance (pc)	ΔR.A. (arcsec)	ΔDecl. (arcsec)	Notes
2M 0010+17	M8	15.2	−0.1	35.1	−12.8	12.3	WIYNa, $I - J = 2.2$, CUT
2M 0015+35	L2	16.9	−1.9	20.1	27.4	−9.3	WIYNa, $I - J = 1.2$, CUT
2M 0028+15	L4.5	16.0	0.0	43.3	9.3	−14.1	WIYNa, $I - J = 1.2$, CUT
2M 0109+29	M9.5	16.2	0.0	18.4	−25.7	31.2	WIYNa, $I - J = 2.7$, CUT
2M 0140+27	M8.5	17.3	0.4	17.3	−14.2	28.4	WIYNa, Elongated, CUT
2M 0208+25	L1	14.8	1.2	69.6	28.2	−14.6	*
2M 0208+25	L1	14.9	1.9	69.6	−26.3	17.9	*
2M 0224+25	L2	15.4	0.8	70.7	30.9	27.7	*
2M 0253+27	M8	15.2	0.9	18.5	2.9	−24.4	WIYNa, $I - J = 1.7$, CUT
2M 0253+27	M8	17.3	0.5	18.5	−11.6	−27.3	WIYNa, $I - J = 1.5$, CUT
2M 0306+15	L6	16.9	0.4	42.0	17.6	0.7	WIYNf, $I - J = 1.5$, CUT
2M 0306+15	L6	16.9	0.0	42.0	16.3	8.5	WIYNf, $I - J = 1.5$, CUT
2M 0306+15	L6	17.0	−0.3	42.0	28.1	6.6	WIYNf, $I - J = 1.4$, CUT
2M 0326+29	L3.5	15.1	1.3	32.3	−24.9	−1.5	*
2M 0409+21	L3	17.2	0.2	37.8	−11.1	−24.1	WIYNa, Elongated, CUT
2M 0409+21	L3	17.0	−1.4	37.8	7.7	14.1	WIYNa, $I - J = 1.0$, CUT
2M 0753+29	L2	15.6	0.4	43.4	−18.9	−11.8	WIYNf, $I - J = 1.2$, CUT
2M 0829+26	L6.5	14.4	0.0	37.3	30.8	28.6	SDSS, $i - z = 0.56$, $z - J = 0.8$, CUT
2M 0856+22	L3	15.3	0.6	39.3	2.8	23.7	SDSS, $i - z = 0.65$, $z - J = 1.34$, CUT
2M 0918+21	L2.5	15.1	1.9	38.4	−21.7	−7.3	SDSS, Not Detected, *
2M 0918+21	L2.5	15.4	1.8	38.4	−6.7	25.0	SDSS, $i - z = 0.28$, $z - J = 1.7$, CUT
2M 1102−23.......	L4.5	15.4	0.8	55.8	2.5	−22.6	*
2M 1146+22	L3	17.8	0.4	27.2	21.1	0.6	WIYNf, Not Detected
2M 1439+18	L1	15.3	1.7	66.8	−12.8	−23.9	SDSS, $i - z = 0.55$ $z - J = 1.23$ CUT
2M 1707+64	M9	19.0	−0.2	16.6	11.3	−17.2	WIYNa, $I - J = −0.5$, CUT
2M 1710+21	M8	14.7	1.0	82.6	20.0	−13.3	SDSS, $i - z = 0.8$ $z - J = 1.03$ CUT
2M 1710+21	M8	14.6	2.1	82.6	−7.6	1.1	SDSS, $i - z = 0.7$ $z - J = 1.26$ CUT
2M 1711+22	L6.5	17.4	−0.7	37.6	29.2	22.0	WIYNa, $I - J = 0.4$, CUT
2M 1728+39	L7	17.6	0.4	20.3	−5.9	35.6	WIYNa, $I - J = 2.2$, CUT
2M 1733+46	M9.5	17.9	−0.7	21.0	20.0	−13.8	WIYNa, $I - J = 1.4$, CUT
2M 1733+46	M9.5	16.6	0.0	21.0	−32.1	−29.0	WIYNa, $I - J = −0.1$, CUT
2M 1743+58	M9.5	15.2	1.0	30.4	−23.4	−12.0	WIYNa, $I - J = 1.5$, CUT
2M 2049−19.......	M7.5	16.9	−0.1	24.1	6.3	−20.1	WIYNa, $I - J = 1.9$, CUT
2M 2140+16	M8.5	18.6	−0.4	21.1	15.1	25.0	WIYNa, $I - J = 1.0$, CUT
2M 2208+29	L2	14.5	0.6	50.5	−1.8	−22.6	WIYNa, $I - J = 2.0$, CUT
2M 2224−01.......	L4.5	19.1	−0.8	11.4	−13.9	18.2	WIYNa, $I - J = 0.9$, CUT

Notes.—SDSS: Object is in SDSS DR5 field. WIYNa: Field observed with WIYN in 2002 August. WIYNf: Field observed with WIYN in 2003 February. All objects detected in either SDSS or with WIYN imaging have colors that are too blue to be consistent with an ultracool dwarf. Objects with asterisks in the notes column are candidates that still require follow-up observations to determine their nature.

late L and later have $I - J$ greater than 3.8. Of the 24 objects observed at WIYN, 23 were detected, 21 with $I - J$ colors less than 2.7, and 2 were discovered to be elongated (Table 2). The remaining object, near 2M 1146+22, was not detected and thus remained a viable candidate.

An additional seven sources are within the field of the Sloan Digital Sky Survey, Fifth Data Release (SDSS DR5). According to Chiu et al. (2006), L and T dwarfs have $i - z$ colors greater than 2 and $z - J$ colors greater than 2.5. Six of the seven sources were detected in DR5 and all have $i - z$ and $z - J$ colors less than 0.8 and 1.7, respectively, and, therefore, are not ultracool companions. This leaves seven candidate companions. Six of these remaining candidates have colors consistent with late-L or L/T transition dwarfs (Fig. 6), and only one with T dwarf colors. The T dwarf is rejected through methane-band imaging, see § 3.3. Thus, our survey is a complete null result for T dwarf companions and nearly complete for L dwarfs. We believe that the remaining objects are most likely not ultracool companions but background stars, given their position in the color-magnitude diagram. Their $J - K$ colors correspond to main-sequence K and M stars (see the right panel of

Fig. 1 in Cruz et al. 2003). Further observations of these final candidates will be obtained at a later date; however, the overall results of the present investigation are not affected significantly by the indeterminate properties of these objects.

3.3. Methane Absorption Test

The one remaining T dwarf candidate is a potential tertiary member of the 2M 1146+22 system, which is a known, near-equal-mass ultracool binary (Koerner et al. 1999). The observed multiepoch Keck fields are too small to cover the new candidate. If a true brown dwarf companion, the candidate would be the faintest known brown dwarf, with an absolute J magnitude of 18.4, approximately 1 mag fainter than the coolest known T dwarfs, such as Gl 570D (Geballe et al. 2001). It would also be the widest known brown dwarf multiple system, with a separation from the known binary of $21''$, or $\sim$570 AU at $\sim$27 pc.

The candidate was imaged in the H_{MK} band and in the narrow 1.7 μm methane-band filter, Spencer 1.7, during an NSFCam run at IRTF in 2004 April. Figure 7 shows a typical late-T dwarf spectrum with the H_{MK} band and Spencer 1.7 filter profiles. The center
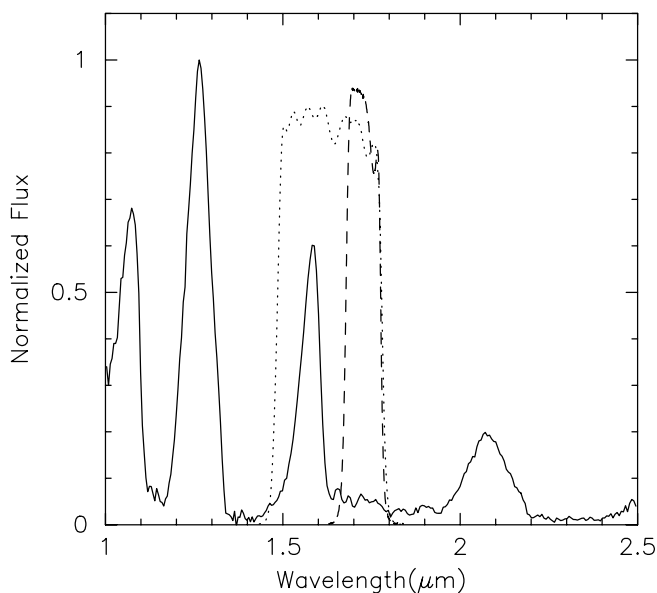
Fig. 7.—Near-infrared spectrum of the T8 dwarf 2M 0415−09 (Burgasser et al. 2002; *solid line*) normalized such that the peak emission (∼1.25 μm) is equal to one, shown with the H_{MK} (*dotted line*) and Spencer 1.7 (*dashed line*) filter transmission profiles. The Spencer 1.7 filter falls in the 1.7 μm methane absorption feature, making the H_{MK}–to–Spencer 1.7 flux ratio indicative of methane absorption.

TABLE 3
$H_{MK}/S17$ Ratios for Known L and T Dwarfs

Spectral Type	Object Name	$H_{MK}/S17$
L2	2M 0015+35	3.5
L4	Gl 165B	3.3
T0	SDSS 0423−04	3.9
T2	SDSS 1254−01	4.2
T5	2M 2254+31	5.8
T6	SDSS 1624+00	7.2
T7	2M 0348−60	11.5
T8	Gl 570D	9.6

Note.—Ratios calculated from published flux calibrated spectra and filter profiles.

of the Spencer 1.7 filter is on the 1.7 μm methane feature that is prominent in cool brown dwarf spectra. Thus, we expect that objects with significant methane absorption will show a drop in flux from H_{MK} to Spencer 1.7.

Table 3 lists the expected H_{MK}/Spencer 1.7 flux ratios, as derived for known L and T dwarfs. The values have been computed from flux-calibrated near-infrared spectra. All T dwarf ratios were calculated from spectra downloaded from Adam Burgasser's T dwarf archive.[1] The L dwarf ratios were calculated from Ian McLean's Brown Dwarf Spectroscopic Survey archive (McLean et al. 2003). The ratio values are flat for L dwarfs (∼3.5) and increase from ∼4 for early-type T dwarfs to ∼11 for the T7 dwarf, 2M 0348−60. If the candidate is a late-type T dwarf, as indicated by its $J − K$ color, then its H_{MK}/Spencer 1.7 flux ratio should be on the order of 10 (Table 3).

To calculate the flux ratio of the candidate, the ratio is calibrated for the main binary system, the L3/L3 2M 1146+22. Since no flux standards were observed, we use flux-calibrated spectra of objects similar to that of the primary. The raw count rate of the primary and the candidate companion were measured at both H_{MK} and Spencer 1.7 using the method described in § 2.2. The measured raw count rate ratio for 2M 1146+22 is 2.2 ± 0.1, and that for the candidate companion is 1.7 ± 1.1. The values derived from flux-calibrated spectra of the L2 dwarf 2M 0015+35 and the L4 dwarf Gl 165B are 3.5 and 3.3, respectively (McLean et al. 2003). These values are about 50% higher than the raw ratio for 2M 1146+22. Hence, the ratio for the candidate is expected to be ∼50% higher, raising it to 2.6 ± 1.1. We surmise that it does not exhibit any significant methane absorption, as would be expected for a very late type T dwarf.

The observed ratio between H_{MK} and Spencer 1.7 for the candidate is also similar to the ratio of the bandwidths of the two filters ($\Delta H \sim 0.35$ μm, $\Delta S \simeq 0.15$ μm), ∼2.3. Since the InSb detectors have a relatively uniform response with wavelength, this is consistent with a flat-spectrum source. It is concluded that

this candidate companion to 2M 1146+22 is not a low-mass brown dwarf companion.

4. DISCUSSION

We have completed a thorough, statistically well-defined search for wide companions to ultracool dwarfs. Previous large-scale surveys (Bouy et al. 2003; Gizis et al. 2003) used optical imaging and concentrated on searching for companions at small separations; our survey is the first to sample the full T dwarf regime at separations from a few tens to thousands of AU. We can calculate an upper limit on the frequency of companions at those separations from our null results. We use a basic Poisson distribution to determine the probability of getting a null detection given the number of observations: Prob(Null) = exp (−N_{obs}Freq), where N_{obs} is the number of observations (132) and "Freq" is the frequency of companions. We determine a conservative upper limit when the probability of obtaining a null result falls below 5%. This occurs at a companion frequency of 2.3%. We will address the issue of overall ultracool dwarf companion frequency with greater detail in a forthcoming paper (Allen 2006).

Since most of the targets of this survey are brown dwarfs, with masses that are dependent on the age of the system, we cannot directly express our results as an upper mass limit on wide companions. However, as discussed in § 2.2, and illustrated in Figure 4, the average K-band limiting magnitude is ∼6 mag fainter than the primary. We can use the magnitude difference to obtain a statistical estimate of the likely limiting mass ratio for each system, $q = M_2/M_1$.

We have transformed the observed magnitude difference to a mass ratio using the Burrows et al. (2001) low-mass star/brown dwarf evolutionary models. The techniques used are similar to those employed in Allen et al. (2005); as in that paper, we transform the theoretical bolometric tracks to the M_K plane using bolometric corrections from Golimowski et al. (2004). Given M_K and ΔK for each source, we estimate the mass ratio detection limit for a range of ages from 20 Myr to 10 Gyr; the result is the detection probability of companions as a function of mass ratio and primary spectral type. This detection probability is a measure of the likelihood that a companion of a given mass ratio can be detected. An observation with a 60% detection probability for a mass ratio of 0.4 means that we would find 60% of the companions with a mass ratio of 0.4. The detection probability increases with increasing mass ratio. For example, 100% of companions with mass ratios between 0.8 and 1 are found in all observations. Figure 8 plots the mass ratio limit as a function of the spectral type at which the detection probability falls below 85% and 50%; the typical values are $q > 0.75$ and $q > 0.45$, respectively. As discussed in Allen et al. (2005), M7–L8 dwarfs are expected to have masses between 0.1 and 0.07 $M_\odot$. Thus, these limits correspond to typical

---

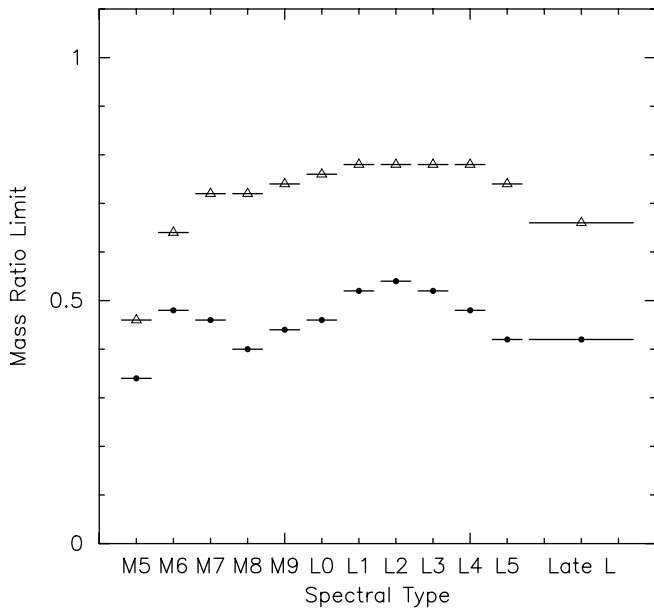[1] See http://web.mit.edu/ajb/www/tdwarf.

Fig. 8.—Predicted minimum mass ratio of detectable companions in the IRTF survey from our modeling as a function of primary spectral type for 85% detection probability (*triangles*) and 50% detection probability (*circles*).

M_{tot}^2 in the range $0.2\ M_\odot > M_{tot} > 0.1\ M_\odot$. This suggests that the absence of wide companions in very low mass systems is the culmination of a continuous, mass-dependent mechanism, rather than a process specific to brown dwarf origins.

To summarize, we find that wide companions to ultracool dwarfs are rare, with a binary frequency upper limit of 2.3%, for companion masses above $0.03-0.05\ M_\odot$. However, these results are one piece of the larger ultracool dwarf companion puzzle. More extensive simulations and theoretical analyses, spanning the full mass range, are required to assess the full implications of the present results for brown dwarf formation scenarios. This issue will be addressed in a future paper (Allen 2006), combining all extant ultracool dwarf companion surveys with observations of binary stars in the solar neighborhood.

companion masses from 0.05 to 0.075 $M_\odot$ at an 85% detection probability and $0.03-0.05\ M_\odot$ at 50%. Deeper imaging is required to probe the full range of potential mass ratios.

The absence of wide companions to ultracool dwarfs has been discussed previously in the literature (Reid et al. 2001; Gizis et al. 2003; Bouy et al. 2003; Burgasser et al. 2003). Our survey extends coverage to lower luminosities and lower mass ratio systems. These results are generally consistent with the ejection scenario for brown dwarf formation (Reipurth & Clarke 2001), where only close, tightly bound binary systems survive the ejection process. However, recent hydrodynamic simulations by Delgade-Donate et al. (2004) suggest that dynamical disruption, rather than ejection, may be sufficient to account for the lack of wide, low-mass systems. Moreover, Burgasser et al. (2003) have compiled data for a wide range of binary systems, and show that there is a correlation between maximum separations, a_{max}, and the total system mass, M_{tot} (see their Fig. 9), at least for $M_{tot} < 1\ M_\odot$. Burgasser et al. also report a possible change in the boundary relation [defining a_{max} as $f(M_{tot})$] from an exponential, $\log a_{max} \propto M_{tot}$, to $a_{max} \propto$

REFERENCES

Allen, P. R. 2006, ApJ, submitted
Allen, P. R., Koerner, D. W., Reid, I. N., & Trilling, D. E. 2005, ApJ, 625, 385
Billères, M., Delfosse, X., Beuzit, J.-L., Forveille, T., Marchal, L., & Martín, E. L. 2005, A&A, 440, L55
Bouy, H., Brandner, W., Martín, E. L., Delfosse, X., Allard, F., & Basri, G. 2003, AJ, 126, 1526
Burgasser, A. J. 2004, ApJS, 155, 191
Burgasser, A. J., Kirkpatrick, J. D., Reid, I. N., Brown, M. E., Miskey, C. L., & Gizis, J. E. 2003, ApJ, 586, 512
Burgasser, A. J., et al. 2002, ApJ, 564, 421
Burrows, A., Hubbard, W. B., Lunine, J. I., & Liebert, J. 2001, Rev. Mod. Phys., 73, 719
Chauvin, G., et al. 2004, A&A, 425, L29
Chiu, K., et al. 2006, AJ, 131, 2722
Close, L. M., Siegler, N., Freed, M., & Biller, B. 2003, ApJ, 587, 407
Close, L. M., et al. 2006, ApJ, submitted (astro-ph/0608574)
Cruz, K. L., Reid, I. N., Liebert, J., Kirkpatrick, J. D., & Lowrance, P. J. 2003, AJ, 126, 2421
Dahn, C. C., et al. 2002, AJ, 124, 1170
Delfosse, X., et al. 1999, A&AS, 135, 41

Delgado-Donate, E. J., Clarke, C. J., Bate, M. R., & Hodgkin, S. T. 2004, MNRAS, 351, 617
Djorgovski, S. G., Carvalho, R. R., Gal, R. R., Odewahn, S. C., Mahabal, A. A., Brunner, R., Lopes, P. A. A., & Kohl Moreira, J. L. 2003, Bol. Soc. Astron. Brasileira, 23, 197
Fan, X., et al. 2000, AJ, 119, 928
Geballe, T. R., Saumon, D., Leggett, S. K., Knapp, G. R., Marley, M. S., & Lodders, K. 2001, ApJ, 556, 373
Gizis, J. E., Monet, D. G., Reid, I. N., Kirkpatrick, J. D., Liebert, J., & Williams, R. J. 2000, AJ, 120, 1085
Gizis, J. E., Reid, I. N., Knapp, G. R., Liebert, J., Kirkpatrick, J. D., Koerner, D. W., & Burgasser, A. J. 2003, AJ, 125, 3302
Golimowski, D. A., et al. 1998, AJ, 115, 2579
———. 2004, AJ, 127, 3516
Hawley, S. L., et al. 2002, AJ, 123, 3409
Kirkpatrick, J. D., Beichman, C. A., & Skrutskie, M. F. 1997, ApJ, 476, 311
Kirkpatrick, J. D., et al. 1999, ApJ, 519, 802
———. 2000, AJ, 120, 447
Koerner, D. W., et al. 1999, ApJ, 526, L25
Kroupa, P. 2002, Science, 295, 82

Luhman, K. L. 2004, ApJ, 614, 398

Martín, E. L., Basri, G., Zapatero-Osorio, M. R., Rebolo, R., & García López, R. J. 1998, ApJ, 507, L41

Martín, E. L., Delfosse, X., Basri, G., Goldman, B., Forveille, T., & Zapatero Osorio, M. R. 1999, AJ, 118, 2466

McLean, I. S., McGovern, M. R., Burgasser, A. J., Kirkpatrick, J. D., Prato, L., & Kim, S. S. 2003, ApJ, 596, 561

Phan-Bao, N., et al. 2003, A&A, 401, 959

Reid, I. N., et al. 2001, AJ, 121, 489

Reipurth, B., & Clarke, C. 2001, AJ, 122, 432

Saha, A., Armandroff, T., Sawyer, D. G., & Corson, C. 2000, Proc. SPIE, 4008, 447

Shure, M. A., et al. 1994, Proc. SPIE, 2198, 614

Siegler, N., Close, L. M., Mamajek, E. E., & Freed, M. 2003, ApJ, 598, 1265

van Biesbroeck, G. 1944, AJ, 51, 61